Int J CARS manuscript No.
(will be inserted by the editor)

Principal Component Vector Rotation of the Tongue Color Spectrum to Predict Mibyou (Disease-Oriented State)

Satoshi Yamamoto · Norimichi Tsumura · Toshiya Nakaguchi · Takao Namiki · Yuji Kasahara · Keiko Ogawa-Ochiai · Katsutoshi Terasawa · Yoichi Miyake

Received: date / Accepted: date

Abstract *Purpose* Kampo medicine (Japanese traditional herbal medicine) contains concepts useful for preventive medicine. For example, Mibyou (disease-oriented state) aims to prevent illness by early recognition. Kampo diagnosis is based on subjective examinations, such as tongue inspection, by trained specialist physicians. An objective metric of the tongue color spectrum was developed as a surrogate for subjective visual inspection.

Methods Tongue images were acquired with a hyperspectral imaging system, and the uncoated tongue region was segmented automatically. The spectral information of the uncoated tongue area was analyzed by principal component analysis (PCA). The component vector most representative of each clinical symptom was found by rotating the vector on a plane spanned by two arbitrary principal component vectors.

Results The system was tested in human volunteers. Forty-four hyperspectral images were acquired from 30 healthy male subjects for initial testing. The Oketsu (blood stagnation) score was determined by an experienced clinician in Kampo medicine from 27 of 30 subjects. The correlation between respective principal components and Oketsu score was 0.67 at maximum, and increased to 0.73 by linear combination, while it was -0.75 by vector rotation. Significant correlations for many disorders were demonstrated, and vector rotation showed better correlation than linear combination.

Conclusions A PCA-based algorithm was developed to objectively evaluate patients using color images of the tongue surface. Testing showed that this method was a feasible surrogate for expert visual tongue analysis. This tool should help non-trained people identify Mibyou health status for individuals. The algorithm is free of empirical criteria, and it may be it applicable to many hyperspectral image types.

Keywords Hyperspectral imaging · Vector rotation · Japanese traditional herbal medicine (Kampo Medicine) · Medical diagnosis · Tongue image analysis

S. Yamamoto · K. Terasawa
Department of Japanese–Oriental Medicine,
Graduate School of Medicine, Chiba University
1-8-1 Inohana, Chuo-ku, Chiba, 260-8670 Japan
Tel.: +81-43-226-2984
Fax: +81-43-226-2985
E-mail: may-s@umin.net (S. Yamamoto)

N. Tsumura · T. Nakaguchi
Graduate School of Advanced Integration Science,
Chiba University
1-33 Yayoi-cho, Inage-ku, Chiba, 263-8522 Japan

T. Namiki · Y. Kasahara
Department of Frontier Japanese–Oriental Medicine,
Graduate School of Medicine, Chiba University
1-8-1 Inohana, Chuo-ku, Chiba, 260-8670 Japan

K. Ogawa-Ochiai
Department of Japanese–Oriental Medicine,
Chiba University Hospital
1-8-1 Inohana, Chuo-ku, Chiba, 260-8677 Japan

Y. Miyake
Research Center for Frontier Medical Engineering,
Chiba University
1-33 Yayoi-cho, Inage-ku, Chiba, 263-8522 Japan

1 Introduction

The appearance of tongue and face, mainly in terms of color, contains a lot of useful information for medical diagnosis, as it is an essential factor for visual examination of Kampo medicine (Japanese traditional herbal medicine) [1, 2]. Details of the problems Kampo is facing are discussed in the first article [3, §1 Introduction]. Also, we showed that uncoated tongue area can be segmented properly by focusing on spectral color difference

among facial areas, which will help analyze tongue color without the effect of tongue coating. In response to this result, we started analyzing the spectral color property of the tongue.

A hyperspectral imaging system for the tongue was previously developed [4–8]. Liu *et al.* developed a hyperspectral camera for tongue diagnosis [5], and they used support vector machines for tongue segmentation [4] and classification [7]. Their segmentation results seem very accurate in their condition; however, they did not focus on specular reflection and shadow removal. Specular reflection and shadow makes the border of the tongue distinct, which will help segmentation. Nevertheless, specular reflection does not represent the color of the tongue but rather the color of the light source. When the tongue image is shown with specular reflection and shadow, even a simple segmentation method with thresholding and extracting the connected area works well, as shown in the first article [3, Fig. 1]. Their classification method was focused on diseases, and that with hyperspectral image has even better performance than that with *RGB* image. Their method is very useful for diagnosis of traditional Chinese medicine where a physician is not present, and is even useful for Kampo medicine. However, the disadvantage of such "classification" method is that they need a database, which is already classified according to empirical criteria. Li *et al.* used a spectral angle mapper (SAM) for tongue segmentation [6] and classification [8]. They used the so-called "SAM cube", constructed for every two adjacent pixels. Although their method works well in their images, they are also not concerned with specular reflection / shadow elimination. Their classification method is focused on tongue color classification. It is also very useful for traditional Chinese medicine and Kampo medicine, but still needs an empirical database. Another criterion is necessary for subjective measurement of the tongue color with continuous quantity.

Therefore, in this article, we focused on the hyperspectral information of the tongue itself, without any empirical considerations, and its correlation to one of the clinical symptoms in Kampo medicine in order to turn the subjective "Mibyou" factor into an objective factor easily determined for a health check-up. This algorithm was presented in 4 steps; 1) hyperspectral tongue images, without specular reflection, were taken by the hyperspectral imaging system equipped with an integrating sphere, 2) tongue area without coating was eliminated according to the spectral properties, 3) the spectral properties of the eliminated uncoated tongue area were converted into spectral absorbance information and directed to principal component analysis (PCA), 4) each component vector was rotated on a plane spanned by two principal component vectors, and the correlation between the clinical symptom and the weight of each component vector was calculated.

2 Hyperspectral Imaging System

The details of the system were shown in the first article [3, §2 Hyperspectral Imaging System].

Forty-four hyperspectral images were acquired from 30 healthy subjects, all male Mongoloids aged 27.9±7.6 years (21–51 years). The images were taken with enough intervals to allow the tongue appearance to change. Because tongue appearance could change with time, images were taken immediately after the tongue was extended. Acquired data were then normalized as spectral reflectance; it was calculated at respective pixels as the ratio of the spectral distribution divided by that of the diffuse reflection standard.

3 Histology of Tongue and Tongue Color Model

Tongue is classified as part of the digestive system and functions as a primary part of the system; it functions not only as taste sensor or for articulation but also for crushing food and mixing saliva — primary digestive fluid and swallowing [9]. Macroscopically, tongue color can be differentiated mainly into two parts, coated area and uncoated area by the presence of tongue coating. That is, the edge and apex seem uncoated in all people, and lamina is coated in most, but not all, as the quantity of coating differs between individuals. On histological sections, the coated area contains the dorsal surface, is covered with filiform papillae that are highly keratinized, the grade of keratinization differing in subjects, presumably the cause of difference in the macroscopic view. In contrast, the uncoated areas contain the edge and apex and are covered with fungiform papillae, which are not keratinized [10].

A multi-layered model has previously been developed for human skin color [11]. In human skin, melanin and hemoglobin are the dominant chromophores, with melanin mainly present in the epidermal layer and hemoglobin in the dermal layer, indicating that human skin should be considered as a multi-layered structure. In contrast, in the tongue, melanin is less, and the mucous epithelium is not lined with a submucosal layer as ordinary mucous, and instead the lamina propria mucosae is lined with lingual aponeurosis, which is tight connective tissue. The lingual aponeurosis is directly connected to lingual muscle. That is, muscle is very near the surface, and the color of muscle and submucosal blood can be seen through a transparent mucous layer.

A schematic model of a tongue is shown in Fig. 1. In the tongue area without coating, epidermis and aponeurosis (dermis in skin) are much thinner than those of the skin, allowing us to inspect the color of submucosal muscle through it. As these layers are thin and contain less pigment, we empirically assumed the uncoated area to be a simple, single-layered turbid medium.

In this kind of medium, spectral reflectance is assumed to result from the spectral absorption characteristics of the resident chromophores. The negative common logarithm of the spectral reflectance is converted to spectral absorbance on the basis of the modified Beer–Lambert law [11].

According to the classics of Kampo medicine, the tongue color varies in two or more dimensions, the pale–thick axis and the red–purple or Oketsu axis. To determine the components related to such axis, principal component analysis was performed for setting the most appropriate component vector to correlate with the diagnosis of Kampo medicine.

4 Tongue Area Extraction

In all images, tongue area without coating was extracted with the algorithm described in the first article [3, §3 Analysis of Hyperspectral Image]. In the images with extraction error, we manually set optimal parameters for respective images, and some errors were corrected manually [3, Fig. 9].

5 Principal Component Analysis of the Tongue Color Spectrum and Correlation Analysis

First, correlation between principal components and Oketsu score — one criterion for diagnosis in Kampo medicine — was determined. The spectral-absorbance hyperspectral image was prepared preliminarily as the negative common logarithm of the spectral-reflectance hyperspectral image. Then the image was processed with a median filter, kernel size = 5, to remove dot noise, and the pixels representing the uncoated tongue area were picked out. In total, over 220,000 pixels containing spectral absorbance data were chosen from all the images. All data were analyzed by an ordinary method of PCA. The principal components are shown in Fig. 2. The cumulative contribution rate from the 1st to the 5th principal components was about 96% (Table 1). Spectral absorbance of the uncoated tongue area was represented as approximately 96% by using the linear combination of five principal components.

Then, the correlation between the principal components and Oketsu score (Table 2, reproduced from [1])

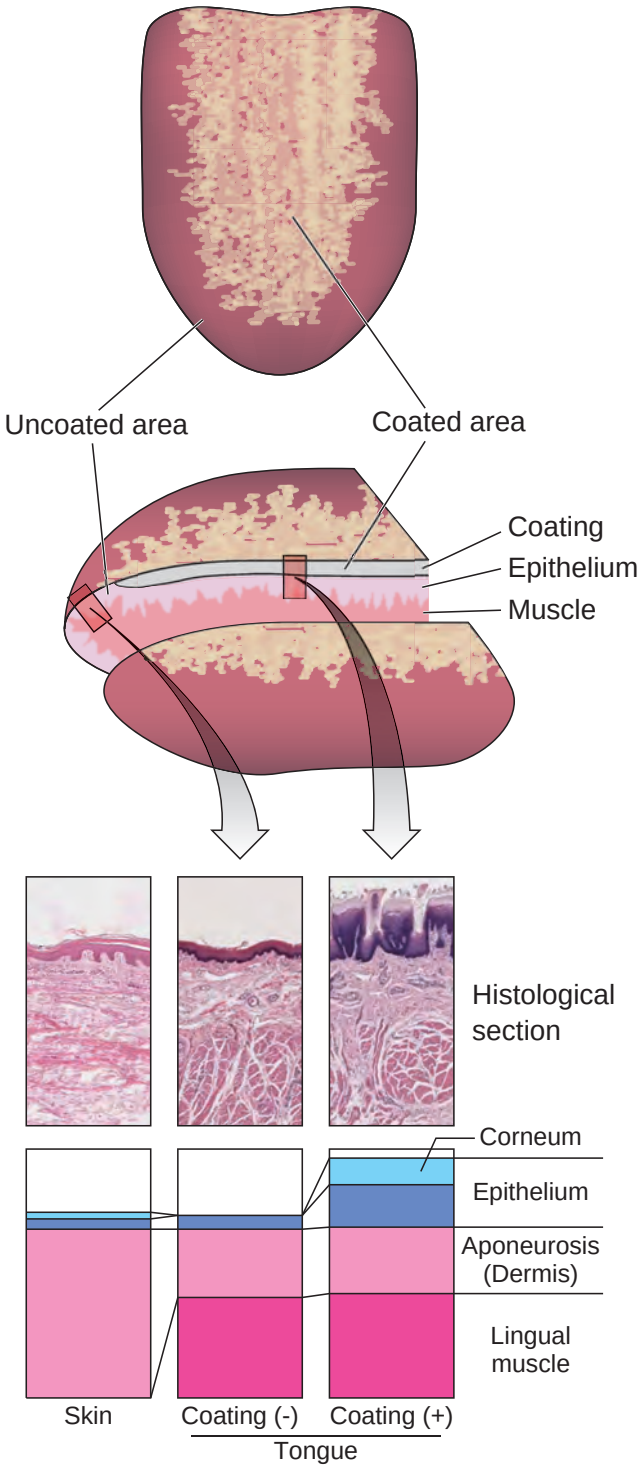

Fig. 1 Schematic drawing of tongue
Scheme of the tongue, image of the histological sections, and scheme of the layers are shown. In the tongue, epidermis is lined with lingual aponeurosis, in contrast to skin that is lined with dermis. Tongue area without coating was assumed to be a single-layered turbid medium, since the mucous layer of the tongue contains less melanin and the subsurface layer is thinner than those of the skin, and is assumed to be a transparent layer.

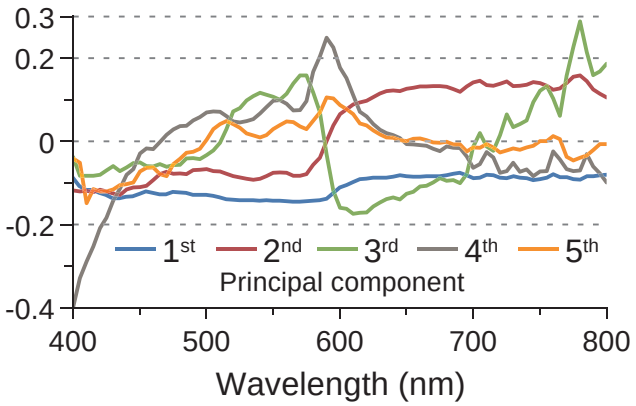

Fig. 2 Principal components of the tongue color spectrum
Principal components of the absorbance spectra of the uncoated tongue area are shown; blue, red, green, gray, and orange lines show the 1st to the 5th principal components, respectively.

	Principal component				
	1	2	3	4	5
Contribution rate	0.70	0.18	0.04	0.03	0.01
Cumulative value	0.70	0.89	0.92	0.95	0.96
	6	7	8	9	10
Contribution rate	0.005	0.004	0.004	0.003	0.003
Cumulative value	0.96	0.97	0.97	0.97	0.98

Table 1 Contribution rate of principal components of the tongue

was analyzed by assessing the weight of each principal component as the component value. The Oketsu score was determined by an experienced clinician in Kampo medicine from 27 subjects who consented to examination.

Component value of each image and principal component was calculated as follows:

$$Cv = -10^{w}, \qquad w = \mathbf{A}_{\lambda} \cdot \mathbf{C}_{\lambda}, \tag{1}$$

where Cv denotes the component value of the image, $\mathbf{A}_{\lambda}$ denotes the absorbance vector (average of spectral absorbance of the selected region), $\mathbf{C}_{\lambda}$ denotes the principal component vector, w is defined as the weight of $\mathbf{C}_{\lambda}$, and $\cdot$ denotes an internal product.

Then, the correlation between Oketsu score and the component value was determined as the linear dependence by computing Pearson's product-moment correlation coefficient. Pearson's correlation coefficient r was calculated as follows:

$$r = \frac{\sum_{i=1}^{n}(K_i - \overline{K})(Cv_i - \overline{Cv})}{\sqrt{\sum_{i=1}^{n}(K_i - \overline{K})^2}\sqrt{\sum_{i=1}^{n}(Cv_i - \overline{Cv})^2}}, \tag{2}$$

where i denotes each subject, n denotes the total number of samples, K_i and Cv_i denote Oketsu score and component value of i-th sample, respectively, and $\overline{K}$ and $\overline{Cv}$ denote the average of Oketsu score and component value, respectively. The result is shown in Table 3.

In the 1st, 2nd, 3rd, 7th, 8th, 9th, and 10th principal components, there were medium, small or no correlations, but a large correlation was shown in the 4th, 5th, and 6th components. Discrete samples with five principal components are shown in Fig. 3.

Then, stronger correlation was determined by multiple linear regression analysis, since respective principal components are independent of each other by their definition. We analyzed three arbitrarily chosen components of ten principal components, respectively, and the combination of the 4th, 5th and 6th principal components showed the best correlation coefficient for the Oketsu score. The best formula derived from the linear

Symptoms	Male	Female
Dark-rimmed eyes	10	10
Areas of dark pigmentation of facial skin	2	2
Rough skin	2	5
Livid lips	2	2
Livid gingiva	10	5
Livid tongue	10	10
Telangiectasis / Vascular spider	5	5
Subcutaneous hemorrhage	2	10
Palmar erythema	2	5
Resistance and/or tenderness on pressure of:		
Right para-umbilical region	5	5
Left para-umbilical region	10	10
Umbilical region	5	5
Cecal region	5	2
Subcostal region	5	5
Right para-umbilical region	5	5
Hemorrhoids	10	5
Dysmenorrhea		10

Table 2 Oketsu score
Oketsu score was previously determined by multivariate analysis conducted between symptoms described in the classics of Kampo medicine and clinical symptoms. Add full points for severe level of symptoms, and half points for moderate level. Oketsu is classified into the three levels by scores of <20 as non-Oketsu, <40 as moderate Oketsu, and ≥40 as severe Oketsu.

	Principal component				
	1	2	3	4	5
Oketsu score	−0.32	−0.32	0.06	0.58	0.68
	6	7	8	9	10
Oketsu score	0.55	0.14	0.39	0.24	−0.07

Table 3 Correlation between principal components and Oketsu score
Pearson's correlation coefficient r is shown. $0 \leq |r| < 0.1$: no correlation, $0.1 \leq |r| < 0.3$: small correlation, $0.3 \leq |r| < 0.5$: medium correlation, $0.5 \leq |r| \leq 1$: large correlation.

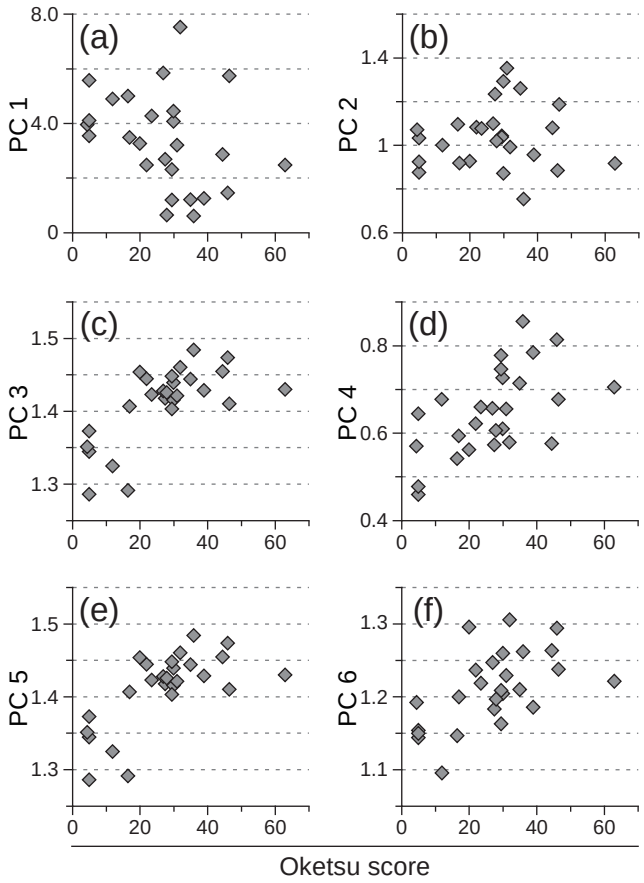

Fig. 3 Correlation between principal components and Oketsu scores
(a)–(f): Component values of the 1st to the 6th principal components (PCs) versus Oketsu score, respectively.

combination of the 4th, 5th and 6th components was as follows:

$$Score = 55.4 \times Cv_4 + 68.2 \times Cv_5 + 73.8 \times Cv_6 - 194.4,$$

where *Score* is the estimated Oketsu score, and Cv_x denotes the component value of the x-th principal component. Multiple correlation coefficient R was 0.73, and determination coefficient R^2 was 0.53. In order to find a vector with even greater correlation, we performed vector rotation as described in the next section.

6 Vector Rotation and Correlation Analysis of Tongue Color

For the next step, the component vector was rotated on a plane spanned by arbitrarily chosen two of the ten principal component vectors in order to define the best component vector to reveal the difference between individuals. The component vector was calculated every two degrees, the component values were calculated for each component vector, and the coefficient of correlation was calculated by Eq. (2). Rotated component vectors were calculated as follows:

The arbitrarily chosen two principal component vectors to span the plane are denoted as $\mathbf{p}_1$ and $\mathbf{p}_2$ and rotated vectors as $\mathbf{r}_1$ and $\mathbf{r}_2$, respectively. It is noted that $\mathbf{r}_1$ and $\mathbf{r}_2$ will span the 81-dimensional plane spanned by $\mathbf{p}_1$ and $\mathbf{p}_2$. $\mathbf{p}_1$, $\mathbf{p}_2$, $\mathbf{r}_1$ and $\mathbf{r}_2$ are normalized as $\|\mathbf{p}_1\| = \|\mathbf{p}_2\| = \|\mathbf{r}_1\| = \|\mathbf{r}_2\| = 1$, where $\|\ \|$ is the Euclidean norm. A schematic diagram is shown in Fig. 4.

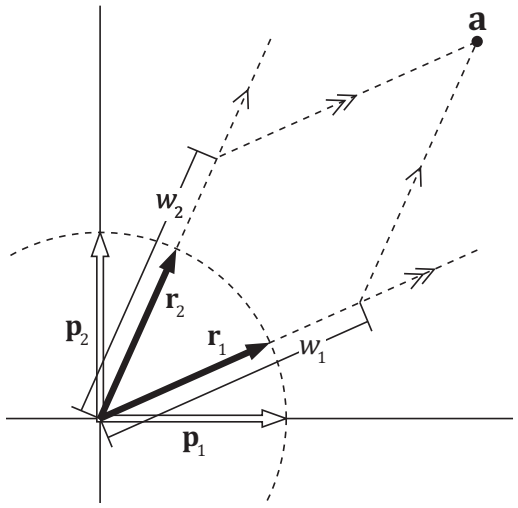

Fig. 4 Schematic diagram of vector rotation
Vectors on the 81-dimensional plane are shown schematically. $\mathbf{p}_1$ and $\mathbf{p}_2$ are arbitrary principal components; they are orthogonal by their definition. $\mathbf{r}_1$ and $\mathbf{r}_2$ are the rotated component vectors on the plane. Note the dashed circle with radius 1. $\mathbf{a}$ is a spectral absorbance vector, and w_1 is the weight of $\mathbf{r}_1$; the distance between the origin to point $\mathbf{a}$ projects an extension of $\mathbf{r}_1$ parallel to $\mathbf{r}_2$. w_2 is the weight of $\mathbf{r}_2$, like w_1.

First, a rotated vector $\mathbf{r}$ was calculated as follows:

$$\mathbf{r} = \mathbf{p}_1 \cos\theta + \mathbf{p}_2 \sin\theta, \tag{3}$$

where θ is an arbitrary angle.

Then a spectral absorbance vector $\mathbf{a}$, representing individual tongue color, is given by

$$\mathbf{a} = \begin{bmatrix}\mathbf{r}_1 & \mathbf{r}_2\end{bmatrix} \begin{bmatrix} w_1 \\ w_2 \end{bmatrix} \quad (\mathbf{r}_1 \nparallel \mathbf{r}_2), \tag{4}$$

where w_1, w_2 are the weight of $\mathbf{r}_1$ and $\mathbf{r}_2$, respectively.

Then Eq. (4) is transposed as

$$\begin{bmatrix} w_1 \\ w_2 \end{bmatrix} = \begin{bmatrix}\mathbf{r}_1 & \mathbf{r}_2\end{bmatrix}^{+} \mathbf{a}, \tag{5}$$

where superscript + denotes pseudoinverse.

To find the Moore-Penrose pseudoinverse matrix, Eq. (6) was employed.

$$\mathbf{X}^{+} = (\mathbf{X}^{t}\mathbf{X})^{-1}\mathbf{X}^{t}, \tag{6}$$

where $\mathbf{X}$ denotes $m \times n$ matrix with Rank($\mathbf{X}$)$= n$, as $\mathbf{r}$ is 81×2 matrix.

Eq. (1), (3), (6) were applied for vector rotation analysis. 10^{w_1} and 10^{w_2}, component values, were calculated for all the images, and correlation between these values and Oketsu score were computed (Table 4). Although correlation was assessed to the 10th principal component, data are shown to the 5th principal component, since the size of the full table was too large and there were no better data than shown in Table 4.

	Principal component			
	2	3	4	5
PC1	−0.44 (54°, 144°)	−0.39 (240°, 24°)	−0.61 (208°, 4°)	0.68 (166°, 180°)
PC2		−0.32 (24°, 70°)	0.60 (222°, 2°)	−0.75 (196°, 4°)
PC3			−0.60 (212°, 0°)	0.69 (170°, 358°)
PC4				0.72 (120°, 352°)

Table 4 Correlation between rotated vectors and Oketsu score (partial data)
The best correlation coefficients on the plane spanned by two each of the principal components are shown in each column. Numbers in parentheses are rotated angles of $\mathbf{r}_1$ and $\mathbf{r}_2$, respectively, as the first principal component (left column) is $\mathbf{p}_1$ and the second principal component (first row) is $\mathbf{p}_2$. Refer to Eq. (3), (4). Partial data are shown because of their large size.

One of the rotated vectors on the principal component 2/5 plane and 4/5 plane showed better correlation than each principal component alone and any linear combination of any three of the ten principal components. Discrete samples with both components are shown in Fig. 5.

7 Discussion

Although the color of the tongue presents a lot of useful information for medical diagnosis, there has not been much research focused on tongue color such as the spectral properties of the tongue, as the diagnostic skills of Kampo medicine have been thought to require great experience in the traditional examination and are not to be substituted. However, those visual examinations need to be objectively evaluated in order to globalize Kampo medicine. Although well-trained Kampo

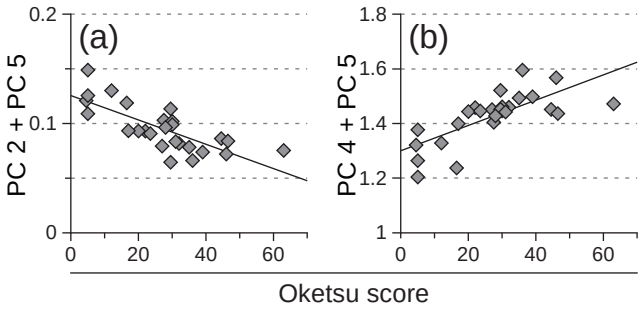

Fig. 5 Correlation between the two best components and Oketsu scores
(a): component values of the best correlated component, $\mathbf{r}_1 = 196°$ and $\mathbf{r}_2 = 4°$ on the plane spanned by the 2nd and 5th principal components versus Oketsu score; (b): component values of the second best correlated component, $\mathbf{r}_1 = 120°$ and $\mathbf{r}_2 = 352°$ on the plane spanned by the 4th and 5th principal components versus Oketsu score.

doctors are proficient in the diagnosis of "Mibyou", it has always been considered that the skills of Kampo medicine must be based on extraordinary levels of experience and education, and those extremely high expectations have restricted the encouragement of the dissemination of Kampo medicine. The hyperspectral imaging system, one of the objective measurement systems available, will help even lesser-trained people to perform this diagnosis of Kampo medicine. However, because a hyperspectral camera presents a major problem in terms of cost [3, §4 Discussion], it is thought that tongue color spectra can be estimated from 3-band images as shown in skin images [11]. If a hyperspectral camera is replaced with a 3-band CCD camera and spectral property of the tongue is estimated for 3-band images, this system would be a new, easily applied, low-cost and noninvasive diagnostic tool for preventive medicine.

In this algorithm, hyperspectral images of the tongue were acquired by the system as shown in the first article [3, §2 Hyperspectral Imaging System]. Using this system, spectral information of the tongue was acquired accurately by eliminating specular reflectance that reflects only color of the color source and contains no information of the subject color. Coating of the tongue, interfering with color analysis by its being stained by colored foods, was clearly removed by the algorithm [3, §3 Analysis of Hyperspectral Image]. The hyperspectral color information of the tongue area without coating was then compressed by PCA, and vector rotation was performed in order to find the best component vector correlated with the Oketsu status, blood stagnation: reflecting serum and blood viscosity [12] or aggregation of red blood cells in capillaries [13], a part of "Mibyou". In Fig. 5, we showed the linear correlation between rotated

components and Oketsu score. As rotated vectors are calculated as shown in Eq. (3), each component value is shown as the linear combination of two respective rotated components. Although vector rotation showed better performance than linear combination of two component vectors, nonlinear combination may have a more precise result, which is our next assignment. In any event, the vector rotation method showed better correlation than linear combination of the principal components by multiple linear regression analysis, and we were able to find the component vector best correlated, which will help "Mibyou" — disease-oriented state — to be detected earlier.

For diagnosis, a tongue color database is frequently employed [8, 14]. These databases originate from the criteria of traditional Chinese medicine, based on subjective inspections by physicians. Additionally, it has been shown that tongue appearance is correlated with certain diseases [14, 15]. For instance, it has been suggested that pancreatitis and appendicitis patients can be recognized by tongue image. We suppose this would be even clearer if detailed color information would be additionally employed.

Hyperspectral tongue image analyses were previously described [7, 8]. Their methods were focused on classification of acquired images into a database created with empirical criteria. Their methods are very useful for diagnosis by traditional Chinese medicine and also for that by Kampo medicine, because their method effectively classified acquired images into the known database that fits the diagnosis of those medical systems. By contrast, our proposed method focuses on the quantification of tongue color. Our method still needs improvement for diagnostic use, but it has the advantage that it is free from a database, and is applicable for comparison with any datum.

On the other hand, although our algorithm has limitations because we are still relying on empirical criteria — Oketsu — as the target, at least our method of color analysis itself is in fact free from such empirical criteria. Currently we are preparing additional data for analyzing the correlation between tongue color and other clinical information, since this experiment was performed preliminarily, before data acquisition in a hospital, and other data such as from blood tests were not able to be acquired from healthy subjects because of ethical issues related to invasive tests.

In this article, tongue area without coating was assumed to be a simple single-layered turbid medium, which helps us assume specular absorbance as the linear combination of pigments. However, as the thin mucous epithelium of the tongue may interfere with the analysis, we are planning to analyze the subsurface scattering effect of this thin layer by such methods as the use of tongue phantom or Monte Carlo simulation method. Furthermore, it is not yet clear what the principal components and rotated vectors represent. We are planning independent component analyses using known spectral absorbance.

Detailed color information has already been examined in respect to the skin. Contents of pigmentation of the face, such as melanin and hemoglobin, can also be estimated by independent component analysis [11, 16]. This analysis is based on the spectral properties of each pigment, and the color of the skin is recovered as the combination of these pigments and shading. Tongue color is also the result of some pigments present in the tongue. Thus, in the next stage, we are not only going to analyze the component vector correlated with the clinical information, but will also search for unknown components related to the contents of tongue pigments.

Our algorithm, hyperspectral tongue image acquisition, principal component analysis, vector rotation and correlation analyses, are applicable not only for the diagnostic criteria of Kampo medicine but also for any data of continuous quantity acquired. We are now collecting more tongue images and more symptoms and data to find new correlations with tongue color.

Even in modern medicine, some physicians examine the tongue whether a patient has anemia or not. Our algorithm enables physicians to obtain more information not only in Kampo medicine or preventive medicine, but also in modern western medicine, if it is proved to have correlation with laboratory data, other clinical images, or clinical manifestations.

8 Conclusion

The correlation between spectral property of the tongue and sign of disease-oriented state was determined and enhanced with PCA and vector rotation method in this study. Tongue area without coating was extracted by the method described in the first article, and spectra of the extracted areas were compressed with PCA. Then, a unit vector was rotated on the plane spanned by arbitrary two principal component vectors, and correlation between rotated vectors and Oketsu score was determined. Experimental results revealed that we could approximate Oketsu scores from the tongue color spectrum without any empirical assessment. Furthermore, this method — PCA and vector rotation — is a generally applicable method for any experiment requiring comparison between spectral properties and subjects. In subsequent studies, we are planning to determine tongue contents that are related to vectors correlated with Oketsu score, estimate spectral properties of the

tongue from 3-band images, and collect more subject images and data to uncover other correlations.

Acknowledgements This work is supported by Joint Industry–Academia–Government Cooperative Project.

References

1. Terasawa K (1993) KAMPO: Japanese–Oriental Medicine — Insights from clinical cases. KK Standard Mclntyre
2. Sato Y, Hanawa T, Arai M, Cyong J, Fukuzawa M, Mitani K, Ogihara Y, Sakiyama T, Shimada Y, Toriizuka K, et al (2005) Introduction to Kampo — Japanese Traditional Medicine. The Japan Society for Oriental Medicine. Tokyo: Elsevier Japan
3. Yamamoto S, Tsumura N, Nakaguchi T, Namiki T, Kasahara Y, Terasawa K, Miyake Y (2010) Regional image analysis of the tongue color spectrum. Int J Comput Assist Radiol Surg (accepted)
4. Liu Z, Yan J, Zhang D, Li Q (2007) Automated tongue segmentation in hyperspectral images for medicine. Appl Opt 46(34):8328–8334
5. Liu Z, Li Q, Yan J, Tang Q (2007) A novel hyperspectral medical sensor for tongue diagnosis. Sensor Review 27(1):57–60
6. Li Q, Xue Y, Wang J, Yue X (2007) Automated tongue segmentation algorithm based on hyperspectral image. J Infrared Millim Waves (Hongwai yu Haomibo Xuebao) 26:77–80, (in Chinese)
7. Liu Z, Zhang D, Yan J, Li Q, Tang Q (2007) Classification of hyperspectral medical tongue images for tongue diagnosis. Computerized Med Imaging Graph 31(8):672–678
8. Li Q, Liu Z (2009) Tongue color analysis and discrimination based on hyperspectral images. Compt Med Imaging Graph 33(3):217–221
9. Snell RS (2003) Clinical Anatomy, 7th edn. Lippincott Williams & Wilkins
10. Kessel RG (1998) Basic Medical Histology: the Biology of Cells, Tissues, and Organs, 1st edn. Oxford University Press, USA
11. Tsumura N, Haneishi H, Miyake Y (1999) Independent-component analysis of skin color image. Journal of the Optical Society of America A 16(9):2169–2176
12. Terasawa K, Toriizuka K, Tosa H, Ueno M, Hayashi T, Shimizu M (1986) Rheological studies on 'Oketsu' syndrome: I. The blood viscosity and diagnostic criteria. J Med Pharmaceut Soc WAKAN-YAKU 3:98–104
13. Terasawa K, Itoh T, Morimoto Y, Hiyama Y, Tosa H (1988) The characteristics of the microcirculation of bulbar conjunctiva in 'Oketsu' syndrome. J Med Pharmaceut Soc WAKAN-YAKU 5:200–205
14. Pang B, Zhang D, Wang K (2005) Tongue image analysis for appendicitis diagnosis. Inform Sci 175(3):160–176
15. Zhang D, Pang B, Li N, Wang K, Zhang H (2005) Computerized diagnosis from tongue appearance using quantitative feature classification. Am J Chinese Med 33(6):859–866
16. Tsumura N, Ojima N, Sato K, Shiraishi M, Shimizu H, Nabeshima H, Akazaki S, Hori K, Miyake Y (2003) Image-based skin color and texture analysis/synthesis by extracting hemoglobin and melanin information in the skin. ACM Trans Graph 22(3):770–779